

Shell-ferromagnetism in a Ni-Mn-In off-stoichiometric Heusler studied by ferromagnetic resonance

Scheibel, Franziska; Spoddig, Detlef; Meckenstock, Ralf; Çakir, Asli; Farle, Michael; Acet, Mehmet

This text is provided by DuEPublico, the central repository of the University Duisburg-Essen.

This version of the e-publication may differ from a potential published print or online version.

DOI: <http://dx.doi.org/10.1063/1.4976335>

URN: <urn:nbn:de:hbz:464-20180108-150613-7>

Link: <https://duepublico.uni-duisburg-essen.de:443/servlets/DocumentServlet?id=45113>

License:



This work may be used under a [Creative Commons Attribution 4.0 International](https://creativecommons.org/licenses/by/4.0/) license.

Source: AIP Advances, 2017, 7, 056425; published online 8 February 2017

Shell-ferromagnetism in a Ni-Mn-In off-stoichiometric Heusler studied by ferromagnetic resonance

Franziska Scheibel,¹ Detlef Spoddig,¹ Ralf Meckenstock,¹ Aslı Çakır,²
Michael Farle,^{1,3} and Mehmet Acet¹

¹*Faculty of Physics and Center for Nanointegration (CENIDE), University of Duisburg-Essen, 47057 Duisburg, Germany*

²*Department of Metallurgical and Materials Engineering, Muğla Sıtkı Koçman University, 48000 Muğla, Turkey*

³*Center for Functionalized Magnetic Materials, Immanuel Kant Baltic Federal University, 236041 Kaliningrad, Russian Federation*

(Presented 1 November 2016; received 23 September 2016; accepted 13 November 2016; published online 8 February 2017)

Next to the multifunctional properties of Ni-Mn-based Heusler alloys new functionalities related to shell-ferromagnetism are emerging. To understand in more detail the properties of shell-ferromagnetism we examine a decomposed $\text{Ni}_{50.0}\text{Mn}_{45.1}\text{In}_{4.9}$ off-stoichiometric compound using magnetic resonance techniques which provides details on magnetic interactions. We find that the ferromagnetic resonance profile of the shell-ferromagnetic state is symmetric for positive and negative fields and is independent of the direction of the field-sweep except for the hysteresis observed at small fields. © 2017 Author(s). All article content, except where otherwise noted, is licensed under a Creative Commons Attribution (CC BY) license (<http://creativecommons.org/licenses/by/4.0/>). [<http://dx.doi.org/10.1063/1.4976335>]

INTRODUCTION

Ni-Mn based Heusler alloys show a broad spectrum of interesting properties like magnetic shape memory, magnetoresistance, and magnetocaloric effects.^{1,2} Depending on the composition, Ni-Mn- X (X : Al, Ga, In, Sn, Sb) Heusler alloys exhibit a first order magneto-structural transition from a low temperature martensite to a high temperature austenite state.³ Alloys close to the stoichiometric Ni_2MnX composition are ferromagnetic (FM), and at more rich Mn compositions, antiferromagnetic (AF) coupling between the Mn-atoms become dominant.⁴⁻⁷ Earlier studies have shown that off-stoichiometric Ni-Mn- X Heusler alloys decompose into a nearly FM Ni_2MnX phase and an AF NiMn matrix when temper-annealed.⁸⁻¹² Temper-annealing between 650 K and 750 K under a magnetic field leads to the growth of Ni_2MnX nano-precipitates with the magnetization of the precipitate-shell being strongly pinned in the direction of the external magnetic field leading to a shell-FM structure. The shell-ferromagnetism causes a vertical shift in magnetization loops $M(H)$ which can be observed at temperatures as high as 450 K; far above the Curie temperature $T_C \approx 320$ K of the FM Ni_2MnX precipitates. On removing the field, the magnetic moments remain pinned. The pinning has been observed to be stable up to applied fields 9 T and up to the annealing temperature. This makes the effect interesting for non-volatile magnetic data storage.^{8,10}

In the present study we investigate ferromagnetic resonance (FMR) and electron spin resonance (ESR) of a decomposed $\text{Ni}_{50.0}\text{Mn}_{45.1}\text{In}_{4.9}$ alloy to understand better the properties of the interface coupling between the shell-FM and the AF matrix.

EXPERIMENTAL

A $\text{Ni}_{50.0}\text{Mn}_{45.1}\text{In}_{4.9}$ alloy was prepared by arc melting under argon. The sample was then sealed in quartz tube under argon atmosphere and annealed at 1073 K for 5 days. The composition and the homogeneity of the sample were checked by energy dispersive x-ray analysis (EDX). Subsequently, the sample was ground to powder and annealed at 1073 K for another day to remove strain. The

sample was then temper-annealed at 650 K in a magnetic field of 4.5 T for 1 hour in a furnace attached to a superconducting quantum interference device (SQUID) magnetometer. FMR and ESR measurements were carried out in a Varian TE102 cavity with an eigen frequency of 9.112 GHz generated by an x-band microwave bridge (Varian E102) using a Varian-E-Line ESR-spectrometer.

RESULTS

Fig. 1 shows $M(H)$ at 300 K for the sample in the initial quenched state (red) and after temper-annealing at 650 K in 4.5 T (blue). The initial tetragonal $L1_0$ state of $\text{Ni}_{50}\text{Mn}_{45.1}\text{In}_{4.9}$ is AF as seen by the essentially linear behavior of $M(H)$. The slight deviation from linearity close to the origin is caused by paramagnetic (PM) inhomogeneities in the sample, which are also detected in the magnetic resonance measurements presented below. $M(H)$ of the annealed sample (blue) is measured after annealing. The field-annealing leads to a vertical shift of the $M(H)$ -curve indicative of the formation of a shell-FM. The FM contribution is extracted from this curve by subtracting the linear $M(H)$ contribution from the AF part. This is shown as the green curve from where it is seen that the FM phase saturates at about 0.19 T. Above this field, the total $M(H)$ (blue curve) runs essentially linear being dominated by the AF matrix-phase. The AF susceptibilities, determined as the slopes of $M(H)$ for the initial and annealed samples, are 1.29×10^{-4} and $1.21 \times 10^{-4} \text{ Am}^2\text{kg}^{-1}\text{T}^{-1}$. The difference reflects the generation of new AF phases when the sample decomposes. $M(H)$ at 10 K (not shown here) gives a saturation magnetization of $0.608 \text{ Am}^2\text{kg}^{-1}$ for the FM part after subtracting the signal from the AF phase. Since $\text{Ni}_{50}\text{Mn}_{25}\text{In}_{25}$ has a saturation magnetization of $80 \text{ Am}^2\text{kg}^{-1}$ at low temperatures,⁷ the amount of $\text{Ni}_{50}\text{Mn}_{25}\text{In}_{25}$ can be estimated to be about 0.072% of the sample.

Magnetic resonance spectra of the initial (red) and the annealed sample (blue) are shown in fig. 2. The solid line is the spectrum for the forward field-sweep from -0.7 T to +0.7 T, and the dashed line is the reverse sweep from +0.7 T to -0.7 T. The sweep-directions are indicated by the arrows. Both spectra show ESR due to a PM phase, while the annealed sample exhibits additionally FMR and a hysteresis in the field range of $-0.05 \text{ T} \leq B \leq 0.05 \text{ T}$.

The initial sample shows only ESR at the symmetric positions $0.338 \pm 0.003 \text{ T}$ on both sides of the origin. Also their width $0.033 \pm 0.003 \text{ T}$ is identical for the positive and negative resonance positions. In combination with the exciting microwave frequency of $9.4630(9) \text{ GHz}$, the resonance field corresponds to a g-factor of 2.0003 ± 0.003 , typical for a nearly free electron. The ESR spectra for forward and reverse sweep-directions are equivalent. The broadening of the resonance can be understood to be due to a superposition of ESR from individual grains and crystallites of the polycrystalline sample, whereby the ESR positions are distributed. The intensity of the ESR is 2.5 times larger than the signal from molecular oxygen in the cavity (not shown in the spectra). Therefore, we can estimate a number of 2.5×10^{18} spins in the initial sample confirming the presence of PM impurities as observed in the magnetization measurements of the initial sample. The AF resonance of $\text{Ni}_{50}\text{Mn}_{45.1}\text{In}_{4.9}$ occurs at higher fields that is not available for this setup.

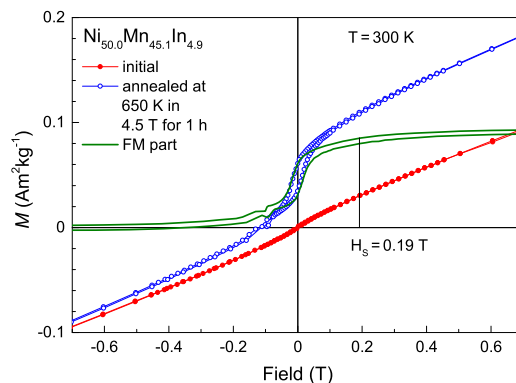


FIG. 1. Field dependence magnetization of initial and annealed $\text{Ni}_{50}\text{Mn}_{45.1}\text{In}_{4.9}$ at 300 K. $\text{Ni}_{50}\text{Mn}_{45.1}\text{In}_{4.9}$ was annealed at 650 K in 4.5 T for 1 hour. The green curve in the estimated FM contribution.

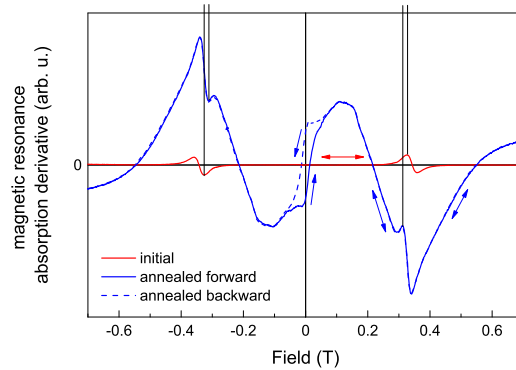


FIG. 2. Magnetic resonance spectra of the initial (red) and annealed (blue) $\text{Ni}_{50}\text{Mn}_{45.1}\text{In}_{4.9}$. The ESR positions are indicated by horizontal lines. The spectrum of the initial sample is reversible. The annealed sample shows irreversibility only in the range of the hysteresis at low fields.

The spectra of the annealed sample (blue) exhibits both ESR and FMR. The effect from the FM phase is more dominant than that from any PM impurity phase as also observed in the magnetization. The resonance field 0.272 ± 0.003 T is identical for positive and negative fields, and also the width 0.125 ± 0.003 T is symmetric around zero-field. The form of the resonance represents a distribution of FMR lines representing each crystallographic orientation in the polycrystalline sample. The ESR in the annealed sample is superimposed on the FMR. The ESR field-positions and widths are, as in the initial sample, equal for negative and positive fields. The width 0.030 ± 0.003 T is equal to that of the ESR of the initial sample, but the field position 0.320 ± 0.003 T is shifted to lower fields. In combination with the exciting microwave frequency $9.127466(9)$ GHz, the resonance field corresponds to a g -factor of 2.038 ± 0.003 which is larger than the g -factor for the initial sample. This indicates that the FM precipitates and the PM parts are interacting. The intensity of the ESR signal corresponds to 4×10^{18} spins. Taking into account that the sample-volume of the initial sample is two times smaller, the number of ESR centers is reduced by the temper-annealing. The spectra of the forward (solid) and backward (dashed) direction of field-sweep are equivalent in the field range of $-0.7 \text{ T} \leq B \leq -0.05 \text{ T}$ and $0.05 \text{ T} \leq B \leq 0.7 \text{ T}$. The deviation of the two spectra in the field range of $-0.05 \text{ T} \leq B \leq 0.05 \text{ T}$ appears as a hysteresis and reflects the hysteresis in $M(H)$. The symmetric values of the field positions of the ESR and FMR is an indication that these resonances are not related to the pinned spins at the interface. They are related to the core of the FM precipitates. The resonance of the pinned spins, as well as the resonances of AF $\text{Ni}_{50}\text{Mn}_{45.1}\text{In}_{4.9}$ and $\text{Ni}_{50}\text{Mn}_{50}$ cannot be detected in this spectra due to their high resonance fields.

CONCLUSION

We studied the magnetic properties of the initial and decomposed, shell-FM states of the $\text{Ni}_{50.0}\text{Mn}_{45.1}\text{In}_{4.9}$ Heusler alloy using magnetic resonance techniques. The magnetic resonance of initial $\text{Ni}_{50.0}\text{Mn}_{45.1}\text{In}_{4.9}$ shows an ESR typical of nearly free electrons caused by the presence of paramagnetic components. The decomposed $\text{Ni}_{50.0}\text{Mn}_{45.1}\text{In}_{4.9}$ contains a FM phase which saturates at 0.19 T. The FMR is symmetric for positive and negative fields and is independent of the direction of field-sweep except for the hysteresis observed at small fields. The ESR of the decomposed sample is shifted due to the coupling between FM and PM states. The effect of shell-ferromagnetism is expected to appear at higher resonance fields which cannot be achieved by the present setup. To detect the resonance of the shell-ferromagnet, further measurements at higher fields are in progress.

ACKNOWLEDGMENTS

Work supported by the Deutsche Forschungsgemeinschaft (SPP 1599).

- ¹ K. Ullakko, J. K. Huang, C. Kantner, R. C. O'Handley, and V. V. Kokorin, *Appl. Phys. Lett.* **69**, 1966 (1996).
- ² I. Dubenko, M. Khan, A. K. Pathak, B. R. Gautam, S. Stadler, and N. Ali, *J. Magn. Magn. Mater.* **321**, 754 (2009).
- ³ M. Acet, L. Mañosa, and A. Planes, in: *Handbook of Magnetic Materials* Vol. 19c, pp. 231 (2011).
- ⁴ Y. Sutou, Y. Imano, N. Koeda, T. Omori, R. Kainuma, K. Ishida, and K. Oikawa, *Appl. Phys. Lett.* **85**, 4358 (2004).
- ⁵ S. Aksoy, M. Acet, E. F. Wassermann, T. Krenke, X. Moya, L. Manosa, A. Planes, and P. P. Deen, *Phil. Mag.* **89**, 2093 (2009).
- ⁶ T. Krenke, M. Acet, E. F. Wassermann, X. Moya, L. Mañosa, and A. Planes, *Phys. Rev. B* **72**, 014412 (2005).
- ⁷ T. Krenke, M. Acet, E. F. Wassermann, X. Moya, L. Mañosa, and A. Planes, *Phys. Rev. B* **73**, 174413 (2006).
- ⁸ A. Cakir, M. Acet, and M. Farle, *Sci. Rep.* **6**, 28931 (2016).
- ⁹ A. Cakir, M. Acet, U. Wiedwald, T. Krenke, and M. Farle, unpublished.
- ¹⁰ T. Krenke, A. Cakir, F. Scheibel, M. Acet, and M. Farle, unpublished.
- ¹¹ D. L. Schlagel, R. W. McCallum, and T. A. Lograsso, *J. Alloys Compd.* **463**, 38 (2008).
- ¹² W. M. Yuhasz, D. L. Schlagel, Q. Xing, R. W. McCallum, and T. A. Lograsso, *J. Alloys Compd.* **492**, 681 (2010).